

# FABRICATION AND ELECTROCHEMICAL PERFORMANCE OF $\text{LiFePO}_4/\text{Ga-LLZO}/\text{Li}$ ALL-SOLID-STATE LITHIUM BUTTON CELL

Ruziel Larmae Gimpaya<sup>1</sup>, Shari Ann Botin<sup>1</sup>, and Rinlee Butch Cervera<sup>1,2</sup>

<sup>1</sup>Energy Engineering Graduate Program, College of Engineering,  
University of the Philippines Diliman, Quezon City, Metro Manila, Philippines

<sup>2</sup>Department of Mining, Metallurgical, and Materials Engineering,  
University of the Philippines Diliman, Quezon City, Metro Manila, Philippines,  
e-mail: rmcervera@up.edu.ph

Received Date: October 21, 2019; Revised Date: August 3, 2020; Acceptance Date: October 16, 2020

## Abstract

An all-solid-state Lithium button cell with Ga-doped  $\text{Li}_7\text{La}_3\text{Zr}_2\text{O}_{12}$  (Ga-LLZO) as solid electrolyte,  $\text{LiFePO}_4$ -based as cathode, and Li metal as anode has been successfully fabricated and characterized. The solid electrolyte was first optimized to obtain a high total conductivity. Different compositions of  $\text{Li}_{7-3x}\text{Ga}_x\text{La}_3\text{Zr}_2\text{O}_{12}$ , where  $x = 0, 0.1, 0.2, \text{ and } 0.3$ .  $\text{Li}_7\text{La}_3\text{Zr}_2\text{O}_{12}$  (LLZO) were synthesized using solid-state reaction and were characterized for its structural, morphological, electrical conductivity properties. XRD patterns of all sintered samples showed that all of the major peaks can be indexed to a cubic-phased garnet LLZO. SEM images revealed a densified sintered samples with relative densities of about 90% for all samples. Among the different studied compositions, the Ga-doped LLZO with  $x = 0.1$  achieved the highest total conductivity of about  $2.03 \times 10^{-4} \text{ Scm}^{-1}$  at  $25^\circ\text{C}$ , with an activation energy of 0.31 eV. From this solid electrolyte, an all-solid-state Lithium battery, 2032 button cell, was fabricated using  $\text{LiFePO}_4$ -based cathode and Lithium metal as the anode. Charging and discharging characteristics were performed at 1C, 0.5C, and 0.2C rates. The results showed a good retention of coulombic efficiency even after 50 cycles of charge and discharge. The capacity retention is about 15-20% after 50 cycles. The best performance of the coin cell battery revealed an initial specific discharging capacity of about 140 mAh/g using C/5 rate.

**Keywords:** All-solid-state battery, Ga-doped LLZO, Lithium battery, Solid electrolyte

## Introduction

All-solid-state Lithium battery is a promising future battery technology that can circumvent the limitations and safety issues of conventional Lithium-ion batteries which typically utilized flammable organic liquid electrolytes. In an all-solid-state batteries, the component electrodes and electrolytes are all made up of solid materials. Some other advantages of using all-solid-state battery, apart from circumventing the safety issues, include: (i) easy miniaturization, (ii) can operate at higher temperature, (iii) higher energy density, and (iv) leakage-free operation. The discovery of solid electrolytes paved the way to the development of this all-solid-state Lithium battery.

Among the solid oxide electrolytes, the garnet-type lithium lanthanum zirconium oxide ( $\text{Li}_7\text{La}_3\text{Zr}_2\text{O}_{12}$  or LLZO) is considered as a promising solid electrolyte because it has the advantages of having excellent stability when in contact with Li metal, high ionic conductivity, and good stability in air [1,2]. However, LLZO only attains good ionic conductivity when it is stabilized in its cubic form [3]. In addition, from literature reports, the ionic conductivity of cubic phased LLZO is two orders of magnitude higher than the more stable tetragonal phase [4, 5]. Various researches have reported that introducing

impurities via doping into LLZO during processing resulted to higher ionic conductivity due to formation of cubic structured LLZO [6]. And one of the promising dopants is Ga which showed promising conductivity [3, 7, 8]. However, only limited reports [9] were published using this Ga-doped LLZO with  $\text{Li}_{7-3x}\text{Ga}_x\text{La}_3\text{Zr}_2\text{O}_{12}$  composition and its electrochemical performance in an all-solid-state battery using  $\text{LiFePO}_4$ -based cathode and Li-metal in a button cell assembly configuration. Hence, in this study, using Ga as dopant in LLZO, different molar concentrations of  $\text{Li}_{7-3x}\text{Ga}_x\text{La}_3\text{Zr}_2\text{O}_{12}$  solid electrolyte ( $x=0, 0.1, 0.2, 0.3$ ) were first synthesized and characterized to obtain the best dopant composition providing a high total conductivity. Then an all-solid state Lithium battery was fabricated using  $\text{LiFePO}_4$ -based cathode and Li metal as anode. The charge-discharge performance and cyclability of the all-solid-state battery were investigated.

## Experimental

### Sample Preparation (Pure And Ga-doped LLZO Solid Electrolyte)

$\text{Li}_{7-3x}\text{Ga}_x\text{La}_3\text{Zr}_2\text{O}_{12}$  (Ga-LLZO) garnets with mole fractions of  $x = 0.0, 0.1, 0.2$  and  $0.3$  were synthesized via conventional solid-state reaction. The precursor materials used were  $\text{LiOH}\cdot\text{H}_2\text{O}$  (98.0%, Unilab),  $\text{La}_2\text{O}_3$  (99.0%, Techno Pharmchem),  $\text{ZrO}_2$  (97.2%, Emfutur), and  $\text{Ga}_2\text{O}_3$  (99.0%, Sigma-Aldrich).  $\text{La}_2\text{O}_3$  was pre-dried at  $900^\circ\text{C}$  for 2 h while  $\text{LiOH}\cdot\text{H}_2\text{O}$  was pre-dried at  $180^\circ\text{C}$  for at least 6 h. Stoichiometric proportions of  $\text{ZrO}_2$ ,  $\text{La}_2\text{O}_3$ ,  $\text{LiOH}$  (+10wt.% to offset Li loss) and  $\text{Ga}_2\text{O}_3$  (for Ga-doped LLZO) were manually ground using agate mortar and pestle with ethanol, and then oven-dried at  $180^\circ\text{C}$ . Calcination was done using a muffle furnace at  $900^\circ\text{C}$  for 2 h at  $10^\circ\text{C}/\text{min}$  heating rate. After cooling, the synthesized powders were reground and oven-dried, and were then pressed into 10 mm diameter pellets using uniaxial pressure of about 20 MPa for 3 minutes (Enerpac high pressure hydraulic cylinder), and sintered using a muffle furnace at  $1150^\circ\text{C}$  for 15 h ( $10^\circ\text{C}/\text{min}$  heating rate). Pellets were covered with mother powder to prevent contamination and avoid loss of volatile components.

### Powder and Pellet Characterization

The X-ray Diffraction (XRD) patterns were collected through Shimadzu MAXima XRD7000 with  $\text{CuK}\alpha 1$  radiation ( $\lambda = 1.54 \text{ \AA}$ ) at a scan rate of  $2 \text{ deg}/\text{min}$  from crushed synthesized samples. The relative densities of the sintered pellets were measured using Archimedes principle by measuring the weight of the pellet in air and when immersed under ethanol to obtain the mass of the displaced fluid. The surface morphologies were observed using Scanning Electron Microscopy (SEM) coupled with Energy-dispersive X-ray Spectroscopy (EDS) mapping. EIS measurements data were collected using Biologic Science Instruments VMP-300 Electrochemical Workstation in the frequency range of 5MHz to 1Hz with a perturbation amplitude of 20 mV in a two-electrode set-up. Ag paste painted on the solid electrolyte and dried at  $150^\circ\text{C}$  was used as the electrode current collector. The resistivity data were graphed in a Nyquist type plot which were analyzed using EC-Lab 10.40 software.

### Fabrication and Coin-cell Assembly (Cathode/SE/Anode)

A thin LLZO solid electrolyte of about 0.3-0.5 mm was prepared. The cathode material was prepared into a slurry and applied on the LLZO pellet via spreading. The cathode was comprised of 50 wt %  $\text{LiFePO}_4$  the active material, 30% LLZO powder as an additive, and 20 wt % carbon black (Emfutur) as the conducting agent. Details of the preparation will be published elsewhere [10].

## Solid State Battery Electrochemical Performance

The electrochemical performance particularly charge-discharge capacities and impedance of the fabricated battery was determined using Biologic™ VMP300 Multi-channel Potentiostat/Galvanostat. Before charging, the impedance of the battery was first tested using the same EIS settings used in the determination of ionic conductivity of LLZO pellet. The working potential used for  $\text{LiFePO}_4$  is 2.2 V to 4.2. V for the charge and discharge capacity testing. After one cycle, the impedance was again determined using the same EIS settings. Cyclability was also tested for 50 cycles.

## Results and Discussion

### Solid Electrolyte Analyses

Different compositions of Ga-doped LLZO were first synthesized using solid state reaction. Figure 1 shows the XRD stacked patterns of the as-sintered samples for undoped LLZO (Figure 1a), 0.1 mol Ga-doped LLZO (Figure 1b), 0.2 mol Ga-doped LLZO (Figure 1c), and 0.3 mol Ga-doped LLZO (Figure 1d). All of the observed major peaks in the XRD patterns for all compositions can be indexed to a cubic phase of garnet LLZO [11].

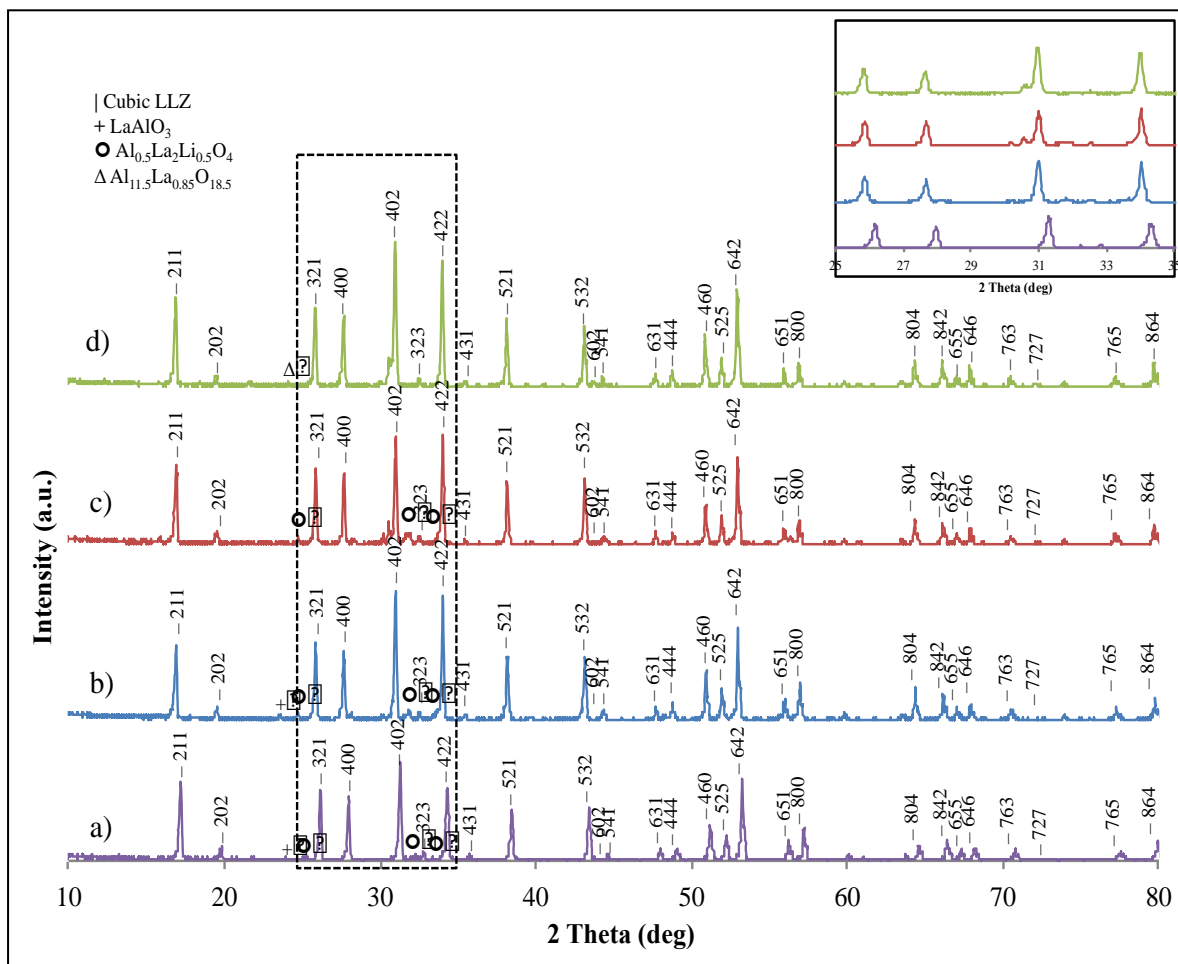


Figure 1. XRD patterns of  $x =$  (a) 0.0, (b) 0.1, (c) 0.2, and (d) 0.3  $\text{Li}_{7-3x}\text{Ga}_x\text{La}_3\text{Zr}_2\text{O}_{12}$  samples, with 10 wt % excess amount of Li source sintered at 1150°C for 15 h

However, some samples, as marked in the pattern, also revealed Al-containing impurity peaks which can be attributed to the formation of  $\text{Al}_{0.5}\text{La}_2\text{Li}_{0.5}\text{O}_4$  (Figure 3a-c),  $\text{LaAlO}_3$  (Figure 3a-b) and  $\text{Al}_{11.5}\text{La}_{0.85}\text{Li}_{18.5}\text{O}_4$  (Figure 3d) [12, 13]. These small impurity peaks can be possibly due to the reaction of the sample with the alumina crucibles that were used during heat treatments.

The calculated lattice parameters are 12.911, 12.914, and 12.926 Å for 0.1, 0.2 and 0.3 Ga-doped LLZO, respectively. These lattice parameters are comparable to the literature lattice parameter value for cubic-phased LLZO sample which is 12.968 Å [2]. It can be noted that a lower value of lattice parameter was calculated due to smaller ionic size of  $\text{Ga}^{3+}$  cation as compared to that of  $\text{Li}^+$  ions (0.62 Å for  $\text{Ga}^{3+}$  vs 0.76 Å for  $\text{Li}^+$  in a 6-coordinated ions). Therefore, upon Ga substitution in the Li-sites, the lattice parameter is expected to decrease.

On the other hand, Figure 2 shows the SEM surface images of the different Ga-doped LLZO compositions. As can be observed from the images, a densified morphology of the sintered samples can be observed, although there are visible pores which are more apparent for the higher dopant compositions.

This is in similar observation for Ga-doped LLZO having few several micrometers pores [14]. However, the calculated relative densities are 88.8%, 86.0%, and 87.4% for the 0.1, 0.2, and 0.3 Ga-doped LLZO, respectively. It can be noted that the relative density is less than 90% due to lower sintering temperature from this study, 1150°C as compared to typical 1200°C [11,14].

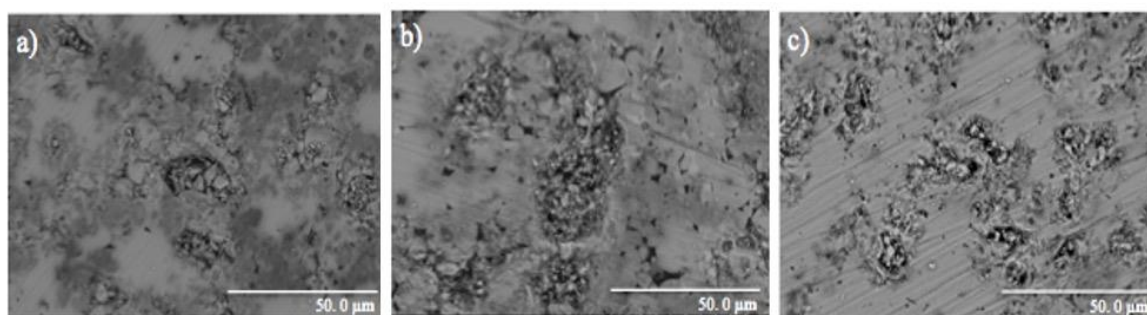


Figure 2. SEM images of  $\text{Li}_{7-3x}\text{Ga}_x\text{La}_3\text{Zr}_2\text{O}_{12}$  with  $x =$  (a) 0.1 (b) 0.2 and (c) 0.3 sintered at 1150°C for 15 h

In order to investigate the effect of dopant concentration and the observed relative densities, the electrical conductivity of the sintered samples was measured using electrochemical impedance spectroscopy.

The synthesized LLZO with 0.1, 0.2 and 0.3 Ga doping have attained ionic conductivities of about  $2.03 \times 10^{-4}$  S/cm,  $5.43 \times 10^{-6}$  S/cm, and  $2.08 \times 10^{-5}$  S/cm, respectively. From these different samples and dopant compositions, LLZO with 0.1 mol Ga achieved the highest total conductivity. The observed  $2.03 \times 10^{-4}$  S/cm conductivity of 0.1 Ga-doped LLZO is comparable to the reported conductivity of  $\text{Li}_7\text{La}_3\text{Zr}_2\text{O}_{12}$  which is  $3 \times 10^{-4}$  S/cm at 25°C [2] and about  $1.3 \times 10^{-3}$  S/cm at 27°C for  $\text{Li}_{0.6}\text{Ga}_{0.2}\text{La}_3\text{Zr}_2\text{O}_{12}$  [15]. Figure 3 shows the Arrhenius-type plot of the total conductivity of the 0.1 mol Ga-doped LLZO. From the slope of this plot, the activation energy,  $E_a$ , is about 0.31 eV in the temperature range of 25-125°C, which is in good agreement with garnet-type solid electrolytes reported in the literature ( $E_a = 0.30$  eV) [3].

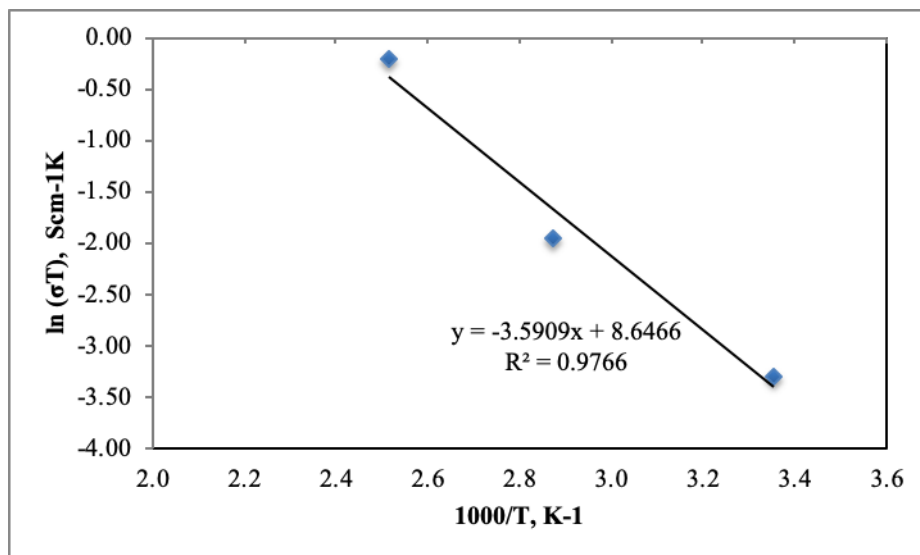


Figure 3. Arrhenius-type conductivity plot of the  $\text{Li}_{7-3x}\text{Ga}_x\text{La}_3\text{Zr}_2\text{O}_{12}$  ( $x = 0.1$ ) sample sintered at  $1150^\circ\text{C}$  for 15 h

### Electrochemical Characterization of the All-solid-state Li Battery Button Cell

Galvanostatic charge-discharge performance of the fabricated all-solid-state lithium battery was tested in the potential range of 2.2 V to 4.2 V (vs.  $\text{Li}^+/\text{Li}$ ) at room temperature. As shown in Figure 4, the charge-discharge performance test ( $C = 0.005$  mA,  $C\text{-rate} = C/5$ ) shows an initial specific charge capacity of  $117.54 \text{ mAh/g}$  and an initial discharge capacity of  $137.92 \text{ mAh/g}$ .

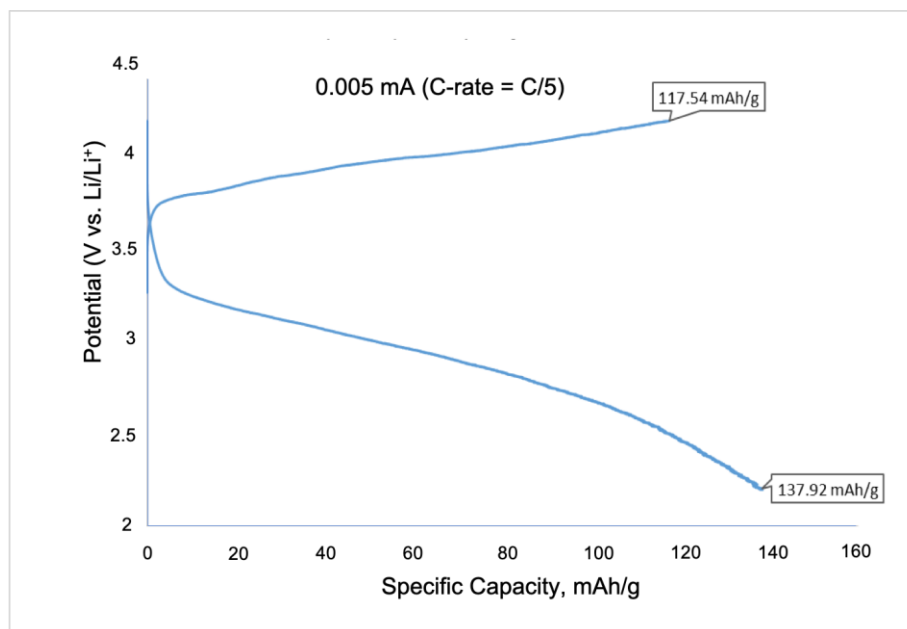


Figure 4. Initial charge and discharge capacity of  $\text{LiFePO}_4/\text{LLZ}/\text{Li}$  battery using  $0.005 \text{ mA}$

The cyclability performance of the fabricated all-solid-state lithium battery was tested at various C-rates:  $1C$ ,  $C/2$  and  $C/5$  and are shown in Figure 5. According to the results, the initial charge capacities at  $1C$ ,  $C/2$  and  $C/5$  rates are  $112.228 \text{ mAh g}^{-1}$ ,  $49.345 \text{ mAh g}^{-1}$ , and  $117.920 \text{ mAh g}^{-1}$ , respectively while the initial discharge capacities are  $82.177 \text{ mAh/g}$ ,

60.029 mAh/g, and 137.920 mAh/g, respectively. The results show a good coulombic efficiency values as the number of cycles increases even up to 10 cycles. On the contrary, it can be noticed that as the number of cycles increases, the capacity values continued to decrease.

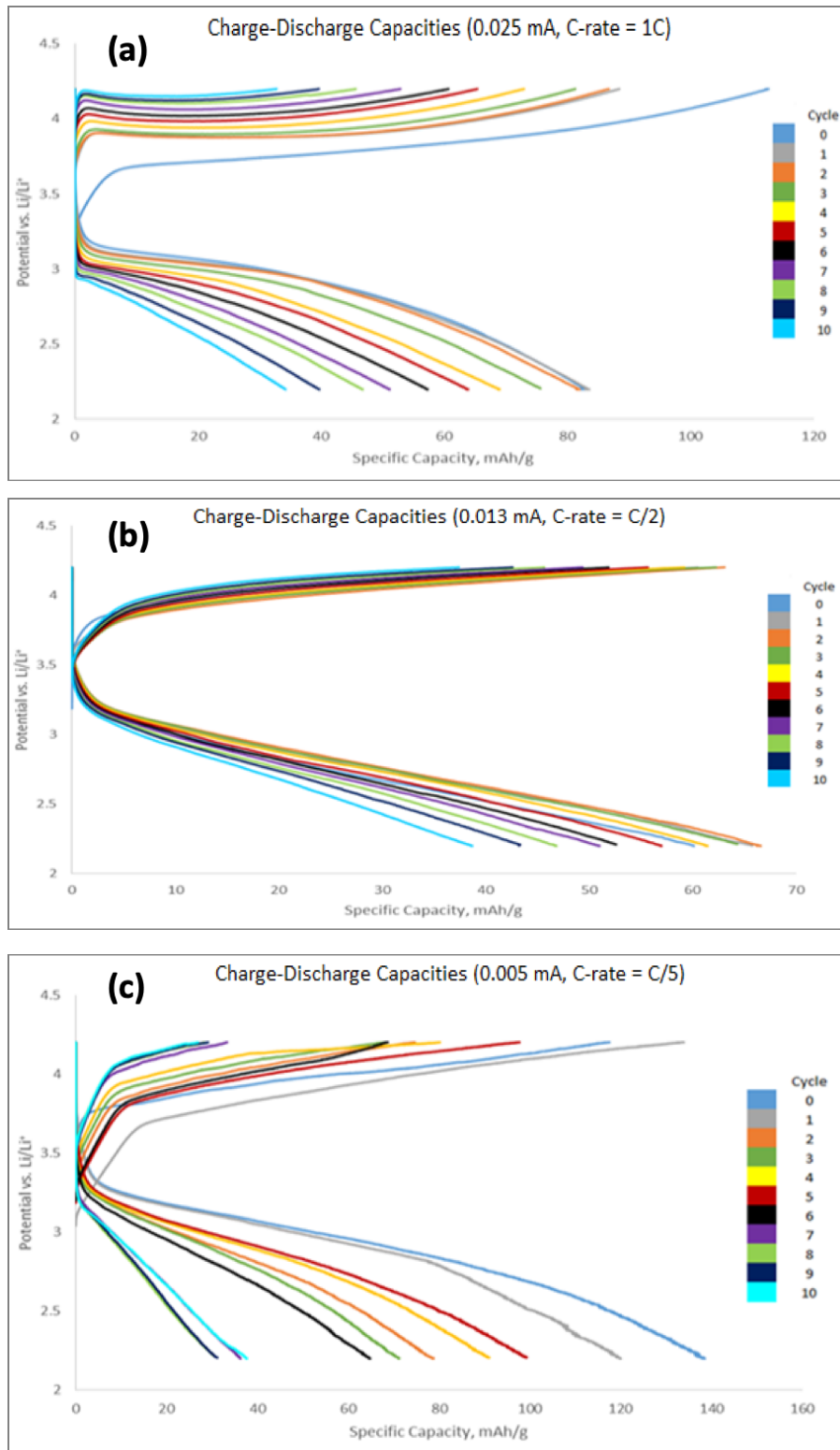


Figure 5. Charge-discharge capacities of all-solid-state battery using (a) 0.025 mA (C-rate = 1C); (b) 0.013 mA (C-rate = C/2); (c) 0.005 mA (C-rate = C/5)

Figure 6a shows the cyclability of the battery using  $C/2$ , capacity from the charge and discharge after 50 cycles. The data revealed the rapid decrease in the capacity from the first cycle up to about 15 cycles and then the capacity does not change much up to 50<sup>th</sup> cycle. It can also be noted that even though the capacity decreases upon cycling, there is still a good coulombic efficiency even after 50<sup>th</sup> cycle. The capacity retention is about 15-20% after 50 cycles.

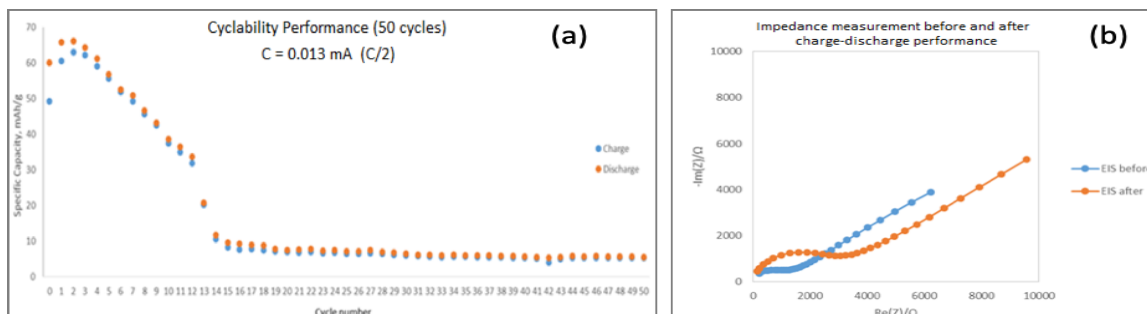


Figure 6. (a) Specific capacity upon cycling up to 50 cycles; (b) Nyquist impedance plot before and after charge-discharge performance

From the literatures, there are only few publications regarding the full cell electrochemical performance of an all-solid-state Lithium batteries using Ga-doped LLZO and its cyclability. Mishra and co-authors in their paper showed about 115 mAh/g specific capacity at 0.1C using a hybrid solid electrolytes of polyethylene oxide, lithium salts and Ga-doped LLZO [11]. This is similar to our reported specific capacity reversible value upon first charge-discharge of about 117 mAh/g as shown in Figure 4. However, there is no cycling performance reported in their study. On the other hand, for pure solid electrolyte, J. Su and co-authors reported a cycling performance of a full cell using Ga-doped LLZO [15]. However, the system is not entirely an all-solid-state Li-battery since the cathode, LFPO on Al foil, was wetted with liquid electrolyte. In their study, a reversible charge/discharge curves of about 150 mAh/g up to 50 cycles were obtained for liquid electrolyte wetted LFPO cathode on Ga-doped LLZO solid electrolyte. In our study and the results reported in this paper, the cathode material is purely in a solid state condition prepared via slurry-coating on the surface of Ga-doped LLZO. In our previous study on half-cell preparations on slurry-coated LFPO on solid electrolyte substrate, the morphology of the deposited cathode is still quite porous using the typical slurry-coating method. From the observed specific capacity and charge/discharge characteristics in Figure 5 and 6, the degradation upon cyclability can be attributed to this porosities that can cause high interfacial resistance and poor pathways for lithium ions. Thus, upon charging, the lithium ion is deintercalated from the LFPO structure and travels to the contact areas between the solid electrolyte to the lithium metal anode; however, during discharging wherein the Li ion is intercalated back, it can be said that this interfacial non-contact between the solid electrolyte and between those particles of LFPO can greatly affect the pathways of lithium ion to intercalate back into the LFPO structure (i.e. irreversible reinsertion of Li-ion to LPFO particle) and vice versa during continued cycling [16]. Hence, this can result to the said observed degradation performance as shown in Figure 6a. It can be said that increasing the cathode densification and good interfacial contact between the cathodes and also with the solid electrolyte can possibly enhance the performance of an all-solid-state Lithium-battery.

Figure 6b shows the Nyquist impedance plot for the first cycle, before and after charge and discharge experiment. It can be observed that the impedance after one cycle increased as shown by the larger semi-circle. This observation is similar to the reported increase in the resistance of LFPO with 50% state of discharge [17], which means that

indeed, it can be said that not all the lithium intercalates back into the LFPO structure, in the assumption that no interfacial layer or resistive oxides have been formed during the first cycle affecting the conductivity. This possible irreversible lithium deintercalation and intercalation in the LFPO structure affects and supports the observed degradation in the electrochemical performance of an all-solid-state lithium battery.

## Conclusions

An all-solid state Lithium button cell has been successfully fabricated using a 0.1 mol Ga-doped LLZO with  $\text{LiFePO}_4$ -based cathode and Li metal anode. The 0.1 mol Ga-doped LLZO solid electrolyte showed a high conductivity value at room temperature of about  $2 \times 10^{-4}$  S/cm among the other different synthesized compositions. The best performance of the coin cell battery revealed an initial specific charging capacity of about 140 mAh/g. Charging and discharging characteristics were performed at 1C, 0.5C, and 0.2C. The button cell also showed and retained its good coulombic efficiency even after 50 cycles of charge and discharge, although the capacity retention is only about 15-20%. Future study is needed to improve the capacities during cycling.

## Acknowledgment

This study was financially supported by PCIEERD-DOST, DOST's grants for outstanding achievements in Science and Technology through the National Academy for Science and Technology (NAST), and by the UP OVPAA Enhanced Creative Work and Research Grant (ECWRG 2018-02-05).

## References

- [1] R.L. Gimpaya, and R.B. Cervera, "Solid-State synthesis and characterization of  $\text{Li}_{7-3x}\text{Ga}_x\text{La}_3\text{Zr}_2\text{O}_{12}$  solid electrolyte for Li-ion battery application," *Key Engineering Materials Journal*, Vol. 705, pp. 145-149, 2016.
- [2] R. Murugan, V. Thangadurai, and W. Weppner, "Fast lithium ion conduction in garnet-type  $\text{Li}_7\text{La}_3\text{Zr}_2\text{O}_{12}$ ," *Angewandte Chemie International Edition*, Vol. 46, pp. 7778-7781, 2007.
- [3] C. Bernuy-Lopez, W.J. Manalastas, J.M. Lopez del Amo, A. Aguadero, F. Aguesse, and J. Kilner, "Atmosphere controlled processing of Ga-substituted garnets for high Li-ion conductivity ceramics," *Chemistry of Materials*, Vol. 26, pp. 3610-3617, 2014.
- [4] Y. Jin, and P.J. McGinn, "Al-doped  $\text{Li}_7\text{La}_3\text{Zr}_2\text{O}_{12}$  synthesized by a polymerized complex method," *Journal of Power Sources*, Vol. 196, No. 20, pp. 8683-8687, 2011.
- [5] R. Sudo, Y. Nakata, K. Ishiguro, M. Matsui, A. Hirano, Y. Takeda, and N. Imanishi, "Interface behavior between garnet-type lithium-conducting solid electrolyte and lithium metal," *Solid State Ionics*, Vol. 262, pp. 151-154, 2014.
- [6] S. Teng, J. Tan, and A. Tiwari, "Recent developments in garnet based solid state electrolytes for thin film batteries," *Current Opinion in Solid State and Materials Science*, Vol. 18, No. 1, pp. 29-38, 2014.
- [7] M. Howard, O. Clemens, E. Kendrick, K. Knight, D. Apperley, P. Anderson, and P. Slater, "Effect of Ga incorporation on the structure and Li ion conductivity of  $\text{La}_3\text{Zr}_2\text{Li}_7\text{O}_{12}$ ," *Dalton Transactions*, Vol. 41, pp. 12048-12053, 2012.
- [8] D. Rettenwander, C.A. Geiger, M. Tribus, P. Tropper, and G. Amthauer, "A synthesis and crystal chemical study of the fast ion conductor  $\text{Li}_{(7-3x)}\text{Ga}_x\text{La}_3\text{Zr}_2\text{O}_{12}$  with  $x = 0.08$  to  $0.84$ ," *Inorganic Chemistry*, Vol. 53, No. 12, pp. 6264-6269, 2014.



- [9] J.F. Wu, W.K. Pang, V. Peterson, L. Wei, and X. Guo, "Garnet-type fast Li-ion conductors with high ionic conductivities for all-solid-state batteries," *Applied Materials and Interfaces*, Vol. 9, pp. 12461-12468, 2017.
- [10] R.B. Cervera, R.L. Gimpaya, S. Botin, and R. Gamboa, *Rechargeable Solid-State Lithium-Ion Battery Using Li<sub>7</sub>La<sub>3</sub>Zr<sub>2</sub>O<sub>12</sub> (LLZO)-Based Garnet as Solid Electrolyte and a Method of Preparing Thereof*, Philippine patent application, 12019050031, 2019.
- [11] Y. Gong, Z.G. Liu, Y.J. Jin, J.H. Ouyang, L. Chen, and Y.J. Wang, "Effect of sintering process on the microstructure and ionic conductivity of Li<sub>7-x</sub>La<sub>3</sub>Zr<sub>2-x</sub>Ta<sub>x</sub>O<sub>12</sub> ceramics," *Solid State Ionics*, Vol. 45, pp. 18439-18444, 2019.
- [12] B.P. Dubey, S. Sahoo, V. Thangadurai, and Y. Sharma, "Morphological, dielectric and transport properties of garnet-type Li<sub>6.25+y</sub>Al<sub>0.25</sub>La<sub>3</sub>Zr<sub>2-y</sub>Mn<sub>y</sub>O<sub>12</sub> (y = 0, 0.05, 0.2, and 0.2)," *Solid State Ionics*, Vol. 351, 2020. Available: <https://doi.org/10.1016/j.ssi.2020.115339>
- [13] D. Rettenwander, R. Wagner, J. Langer, M.E. Maier, M. Wilkening, and G. Amthauer, "Crystal chemistry of Li<sub>7</sub>La<sub>3</sub>Zr<sub>2</sub>O<sub>12</sub> garnet doped with Al, Ga, and Fe: A short review on local structures as revealed by NMR and Mößbauer spectroscopic studies," *European Journal of Mineralogy*, Vol. 28, pp. 619-629, 2016.
- [14] X. Xiang, Liu, Y., F. Chen, W. Yang, J. Yang, X. Ma, D. Cheen, K. Su., Q. Shen, and L. Zhang, "Crystal structure and lithium ionic transport behavior of Li site doped Li<sub>7</sub>La<sub>3</sub>Zr<sub>2</sub>O<sub>12</sub>," *Journal of the European Ceramic Society*, Vol. 40, pp. 3065-3071, 2020.
- [15] J. Su, X. Huang, Z. Song, T. Xiu, M. Badding, J. Jin, and Z. Wen, "Overcoming the abnormal grain growth in Ga-doped Li<sub>7</sub>La<sub>3</sub>Zr<sub>2</sub>O<sub>12</sub> to enhance the electrochemical stability against Li metal," *Ceramics International*, Vol. 45, pp. 14991-14996, 2019.
- [16] K. Inoue, S. Fujieda, K. Shinoda, S. Suzuki, and Y. Waseda, "Chemical state of iron of LiFePO<sub>4</sub> during charge-discharge cycle studied by in-situ X-ray absorption spectroscopy," *Materials Transactions*, Vol. 51, No. 12, pp. 2220-2224, 2010.
- [17] C. Wang, and J. Hong, "Ionic/Electronic conducting characteristics of LiFePO<sub>4</sub> cathode materials," *Electrochemical and Solid State Letters*, Vol. 10, No. 3, pp. A65-A69, 2007.